

Character and environmental lability of cyanobacteria-derived dissolved organic matter

Claudia Patriarca,¹ Vicente T. Sedano-Núñez ,² Sarahi L. Garcia ,^{3,4} Jonas Bergquist,¹ Stefan Bertilsson ,^{3,5} Per J. R. Sjöberg,¹ Lars J. Tranvik ,³ Jeffrey A. Hawkes ^{1*}

¹Analytical Chemistry, Department of Chemistry – BMC, Uppsala University, Uppsala, Sweden

²Molecular Evolution, Department of Cell and Molecular Biology, Science for Life Laboratory, Biomedical Centre, Uppsala University, Uppsala, Sweden

³Limnology, Department of Ecology and Genetics, Uppsala University, Uppsala, Sweden

⁴Department of Ecology, Environment, and Plant Sciences, Science for Life Laboratory, Stockholm University, Stockholm, Sweden

⁵Department of Aquatic Sciences and Assessment, Swedish University of Agricultural Sciences, Uppsala, Sweden

Abstract

Autotrophic dissolved organic matter (DOM) is central to the carbon biogeochemistry of aquatic systems, and the full complexity of autotrophic DOM has not been extensively studied, particularly by high-resolution mass spectrometry (HRMS). Terrestrial DOM tends to dominate HRMS studies in freshwaters due to the propensity of such compounds to ionize by negative mode electrospray, and possibly also because ionizable DOM produced by autotrophy is decreased to low steady-state concentrations by heterotrophic bacteria. In this study, we investigated the character of DOM produced by the widespread cyanobacteria *Microcystis aeruginosa* using high-pressure liquid chromatography—electrospray ionization—high-resolution mass spectrometry. *M. aeruginosa* produced thousands of detectable compounds in axenic culture. These compounds were chromatographically resolved and the majority were assigned to aliphatic formulas with a broad polarity range. We found that the DOM produced by *M. aeruginosa* was highly susceptible to removal by heterotrophic freshwater bacteria, supporting the hypothesis that this autotroph-derived organic material is highly labile and accordingly only seen at low concentrations in natural settings.

Dissolved organic matter (DOM) is a ubiquitous and heterogeneous mixture that is so complex that even the most advanced techniques are unable to completely disclose its molecular composition (Hertkorn et al. 2008; Koch et al. 2008). The organic carbon pool in aquatic ecosystems derives both from terrestrial sources (allochthonous) and internal primary production (autochthonous), and also undergoes transformation and decomposition processes within the aquatic system (Toming et al. 2013). The bulk of DOM in lakes is typically relatively recalcitrant with half-lives of months to years (Amon and Benner 1996; Koehler et al. 2012; Kothawala et al. 2012), while freshly produced autochthonous DOM is generally

thought to be more labile and rapidly turned over (Maki et al. 2010; Bittar et al. 2015b).

The dynamics of the various sources and sinks of DOM in aquatic systems are difficult to unravel with experiments and observations. Studies to date that attempt to quantify the relative importance of allochthonous and autochthonous sources generally use spectroscopic techniques (McKnight et al. 2001), or bulk characteristics like isotope ratios (Toming et al. 2013; Osburn et al. 2019), all of which are techniques that integrate a vast molecular diversity.

The majority of the mass spectrometry research in DOM has so far had a focus on the terrestrial (allochthonous) carboxyl-rich portion, largely due to its high abundance, easy extraction, and propensity to ionize in negative mode electrospray. The lesser characterized autochthonous DOM is nevertheless of extreme biogeochemical importance since it is biologically labile and therefore responsible for a significant fraction of the combined microbial respiration and energy flow in most aquatic ecosystems (Gonsior et al. 2019; Zhou et al. 2019). The study of this DOM fraction is challenging for several reasons. First, its rapid consumption constrains in situ

*Correspondence: jeffrey.hawkes@kemi.uu.se

This is an open access article under the terms of the Creative Commons Attribution License, which permits use, distribution and reproduction in any medium, provided the original work is properly cited.

Additional Supporting Information may be found in the online version of this article.

concentrations and there is rarely any significant concentration build-up over time. Second, some known compounds released by microbial autotrophs, including sugars and peptides, are very hydrophilic and hence not retained by the commonly used solid-phase extraction techniques (Perminova et al. 2014; Raeke et al. 2016). Third, autochthonous DOM is not necessarily rich in the carboxylic acid groups that are characteristic for terrestrial DOM, and may therefore not ionize well in negative mode electrospray.

Mass spectrometry coupled to liquid chromatography has the potential advantage of detecting individual analytes (metabolites) produced by autotrophs (Petras et al. 2017), but has so far not been used for comprehensive characterization of autochthonous DOM in aquatic systems. However, a few recent studies have begun to use high-resolution mass spectrometry in direct infusion mode, enabling detection of a wide range of compounds produced by microbes (Osterholz et al. 2015; Bai et al. 2017; Gonsior et al. 2019). These previous efforts have shown that primary producers generate compounds with hundreds to thousands of different molecular formulas, but due to the lack of chromatography or other modes of separation prior to infusion, the isomeric complexity of the mixture cannot be assessed.

Each molecular formula determined by direct infusion mass spectrometry may represent a multitude of possible structural isomers and the absence of the third dimension able to reduce the sample complexity and the isomeric averaging of the sample prevents robust disclosure of structural information. The combination of chromatography and high-resolution mass spectrometry provides more complementary information for DOM characterization by increasing the total number of assigned formulas due to decrease of ionization suppression (Patriarca et al. 2018). It also provides polarity information on the eluting material and grants the opportunity to isolate individually eluting components (Woods et al. 2011; Petras et al. 2017).

Cyanobacteria-derived DOM represents a potentially important source of autochthonous material and its role may rapidly gain more importance due to increasing global temperatures and nutrient concentrations which favor the spread and blooms of these bacterial phytoplankton, often associated with release of toxins (Paerl and Otten 2013; Gonsior et al. 2019). *Microcystis aeruginosa* is one of the most well-known bloom-forming freshwater cyanobacteria and is widespread in eutrophic lakes, where it commonly forms dense populations (Oliver and Ganf 2000) that are often harmful due to the production of toxic cyclic peptides such as Microcystin-LR. These toxic bloom events are predicted to increase in coming decades (Wells et al. 2015), and their consequences on the carbon cycle and the production of safe drinking water are still unclear (Ritson et al. 2014; Gonsior et al. 2019).

Eutrophication can lead to sequestration of CO₂ in lakes (Pacheco et al. 2014), but the nature of the DOM resulting

from such carbon fixation and its subsequent processing by heterotrophic bacteria has rarely been investigated (Bittar et al. 2015b). In marine settings, autotrophic DOM has been shown to rapidly transform into complex DOM (Aluwihare et al. 1997; Lechtenfeld et al. 2015; Osterholz et al. 2015; Powers et al. 2019). The studies cited differed on whether the resulting DOM resembled stable marine DOM, and this is still an active and controversial debate in biogeochemistry.

In this study, the molecular composition of ionizable DOM derived from *M. aeruginosa* was investigated under two growth conditions using an ultrahigh pressure liquid chromatography-electrospray ionization-high resolution mass spectrometry (UPLC-ESI-HRMS) method. Cyanobacterial cells were grown in axenic cultures and the chemodiversity of the produced dissolved organic material was explored in exponential and stationary phase. In further experiments, we assessed the bioavailability and fate of this autochthonous DOM material in natural surface water settings.

Materials and methods

Microcystis aeruginosa incubation treatments

An axenic culture of *M. aeruginosa* strain PCC-7941 was obtained from the Pasteur Culture Collection of Cyanobacteria (Pasteur Institute, Paris, France). *M. aeruginosa* was first acclimated in BG11 medium (Stanier et al. 1971) in Nunc™ Nontreated Flasks (ThermoFisher Scientific) with filter caps. Subsequently, two different media were used to grow *M. aeruginosa* in acid-washed autoclaved conical culture flasks covered with cellulose stoppers and aluminum foil. For the first treatment (*artificial*), the cyanobacterial cultures were grown in BG11₀ medium (Rippka et al. 1979), a detailed composition of the medium is available in Supporting Information Table S1. The axenicity of the cultures was confirmed by culturing aliquots of our replicates in plates with BG11 solid growth medium (10 g L⁻¹ Bacto Agar, BD Diagnostics, Maryland, U.S.A.) under temperature and light conditions corresponding to our experiment. After 4–5 d of incubation, the shape and color of colonies in the plates were visually analyzed and 2–3 colonies were picked for examination with phase contrast microscopy using a ×100 objective. For the second treatment (*natural*), *M. aeruginosa* cells were grown in filtered lake water at 20°C. Lake water used for incubation was collected from the meso-eutrophic lake Erken, Sweden (59°51'N, 18°36'E), which features yearly *Microcystis* blooms. Surface water was sampled before the spring bloom on 02 April 2019 (2.5°C, pH 7.5), and the water was filtered in an open indoor space through a 0.1 μm hollow fiber cartridge (GE Healthcare, U.S.A.). To ensure removal of possible contamination introduced in the open indoor space, a second filtration was performed in a laminar flow cabinet with a 0.22 μm Sterivex-GP pressure filter (Merck, Darmstadt, Germany). All culture related work was carried out in a laminar flow bench and general aseptic microbiological techniques were used.

All treatments were carried out in triplicate in 1-liter conical culture flasks with a total working volume of 600 mL (540 mL medium and 60 mL inoculum). The cultures were incubated at 20°C with a photon flux density of 25 $\mu\text{mol m}^{-2} \text{s}^{-1}$ and a photoperiod of 12 : 12 h light : dark (Philips TL-D 18&30W 865 Super 80) and rotary shaking at 90 rpm (VWR DS-500 Digital Orbital Shaker & Gerhardt Orbital Shaker RO 10). The purity of the incubations was verified with negative growth controls by placing an aliquot (0.5 mL) of each replicate onto BG11 solid growth medium plates supplemented with glucose (0.2 g L⁻¹) and casamino acids (0.02 g L⁻¹). These plates were incubated in a dark box simultaneously with the treatments at the corresponding growth temperature; visual examination was performed 5 d after incubation. Treatments samples were collected in a laminar flow cabinet regularly over a period of 25 d (*artificial*) or 23 d (*natural*) by collecting 20 mL of solution and filtering the culture through precombusted 0.7 μm glass fiber filters (Whatman GF/F). The filtrate was further passed through a 0.2 μm polyethersulfone syringe filter (Merck, Darmstadt, Germany) prerinsed with 5 mL deionized water (MilliQ, Millipore), and divided in aliquots to determine dissolved organic carbon (DOC) concentration by catalyzed combustion (Shimadzu TOC-L/TNM-L, calibrated with ethylenediaminetetraacetic acid) and DOM character by UPLC-HRMS analysis. *Microcystis* cells (2–5 μm) retained on GF/F filters were used for organic carbon determination using an elemental combustion system (Costech Instruments, Cernusco s/Nav, Italy). These particulate carbon data were used to create growth curves. Additional information related to growth curves, nonpurgeable organic carbon concentrations and dissolved total nitrogen (TN) are available in Supporting Information Table S2. All samples were stored at –20°C until the day of the analysis. In the rest of the article, nonpurgeable organic carbon is referred to as DOC.

Incubation of heterotrophic bacteria in cyanobacteria-derived DOM

In order to assess the biological lability of the DOM produced by *M. aeruginosa* in the *artificial* treatment, an additional experiment (*lability test*) was performed. The triplicate samples collected from the *artificial* treatment at day 25 of incubation were combined after the filtration process described above (GF/F and polyethersulfone filtration). This cyanobacterial-derived DOM was concentrated with a rotary evaporator at about 40°C (0.12 mg total). DOM begins to degrade hydrothermally about 70°C, so we do not expect that this preparation step greatly affected the samples (Hawkes et al. 2016). In order to monitor the cyanobacteria-derived DOM turnover by heterotrophs, unfiltered lake water (from Lake Erken, sampled 11th September 2019, 18.3°C, pH 8.3) was used to reconstitute the sample (12 mL, to make 10 ppm cyanobacteria-derived DOM and ~ 10 ppm lake DOM). No pH adjustment was made. The transformations induced by the endemic heterotrophic bacterial communities present in the

lake water were observed over an incubation period of 14 d (samplings on 0, 2, 5, 7, and 14 d). The experiment was performed in the dark at constant temperature (20°C). Aliquots (500 μL) for DOM characterization were collected, filtered using 0.2 μm polyethersulfone syringe filters (Merck, Darmstadt, Germany), and stored at –20°C until the day of the analysis.

Sample pretreatment and UPLC-HRMS analysis

To maximize the instrument response, a preconcentration procedure was necessary. Solid phase extraction was avoided to maintain the sample integrity (e.g., avoid loss of low molecular weight ionizable material; Cortés-Francisco and Caixach 2013) sample aliquots (500 μL) were transferred to 2 mL Eppendorf vials and dried in a vacuum centrifuge (Savant ISS110) at about 40°C. A concentration factor of 10 was obtained by recovering the dehydrated samples with 50 μL of a 5% acetonitrile solution enriched with 0.1% formic acid and model compounds (Hippuric acid, Fraxin, Capsaicin; 200 ppb in *artificial* and *natural* incubation and Hippuric acid, Fraxin, Glycyrrhizic acid; 500 ppb in the *lability test* experiment) employed to monitor HRMS instrument performance over the analysis time. To ensure complete recovery of the organic material, all samples were sonicated and centrifuged after the solvent addition, and finally transferred to precombusted insert vials (250 μL) suitable for the chromatographic system. A solvent blank was also analyzed in triplicate to determine blank peaks, and growth medium was used to remove blank peaks for the *artificial* treatment samples, while a lake Erken water sample was used to determine background (noncyanobacteria-derived DOM) peaks from the *natural* treatment samples. An Acquity ultra-performance liquid chromatographic (UPLC) instrument (Waters, Milford, Massachusetts, U.S.A.) fitted with a Kinetex polar-C18 column (100 \times 2.1 mm, 2.6 μm ; Phenomenex) was employed for the separation. The UPLC system was equipped with a thermostat for the autosampler and a column oven, allowing sample refrigeration (5°C) and maintaining the column at constant temperature (40°C) for the duration of the analysis. Ten microliters of sample was injected and analytes were separated in a gradient consisting of (A) 18 M Ω cm⁻¹ deionized water (MilliQ, Millipore), 0.1% formic acid and (B) 80% acetonitrile, 0.1% formic acid in water. A 20 min gradient elution program at constant flow rate (250 $\mu\text{L min}^{-1}$) was applied. After the injection, the initial mobile phase composition consisting of 1% B was maintained for 1.5 min, eluent B percentage was then increased to 99% over 18.5 min and held isocratic until 23 min. At min 23.2, the initial mobile phase composition (1% B) was restored and kept constant for additional 9 min to allow the equilibration of the column. Due to sample heterogeneity, a blank injection was frequently performed in order to monitor and reduce potential carryover. A set of standards was also injected to determine the relationship between the elution time and the estimated octanol : water partition

coefficient of the analyte, as well as to assess possible drifting in retention time related to disruption of the column chemistry associated to the amount of organic material introduced (Supporting Information Figure S1).

The UPLC system was coupled to a Q-Exactive Orbitrap (Thermo Scientific, Germany) equipped with a heated-electrospray ionization source (HESI-II, Thermo Scientific) operated in negative mode. External calibration of the mass analyzer was performed on the day of the analysis as specified by the manufacturer's guidelines by using the negative calibration solution (Pierce, Thermo Fisher). The following electrospray settings were used: capillary temperature 300°C, HESI-II vaporizer temperature 280°C, spray voltage -2.5 kV, sheath gas 35 psi, auxiliary gas 10 (arbitrary units), S-lens RF level 50. Spectra were recorded between m/z 120–1000 at 70,000 resolution settings (at m/z 200) with an overall mass accuracy of < 5 ppm over the range of interest (m/z 120–700). The automatic gain control setting was used to trap 1×10^6 ions in a curved linear trap (C-trap) before the ions could be transferred to the Orbitrap. The maximum accumulation time was set to 50 ms. The raw files were exported and converted into mzXML format. The data were finally analyzed with MATLAB R2017b (The MathWorks, Natick, Massachusetts, U.S.A.) using an in-house built script.

Formula assignment and data analysis

In Matlab, mzXML files were unpacked and processed in a series of loops to assign formulas to signals. Spectra were assigned formulas if the elution time was between 2 and 17 min, and signals were assigned if they had $m/z > 120$ and were more intense than $5\times$ the determined noise threshold, which was calculated as the 95th percentile of peaks with mass defect 0.7–0.8. This detection limit is more conservative than some recent approaches (Riedel and Dittmar 2014; Patriarca et al. 2018), but was necessary to reduce the amount of data in this sample set.

A theoretical formula list was generated using combinations of C (4–40), H (4–80), O (0–35), N (0–1), S (0–1), and ^{13}C (0–1). Many formulas were removed from consideration according to the following rules: m/z 120–700, H/C 0.3–2.4, O/C ≤ 1 , double bond equivalence minus oxygen ≤ 10 , formula must be valence neutral, $N + S + ^{13}\text{C} \leq 1$. After these restrictions, a list of known metabolite formulas was added (Zheng et al. 2017) to the theoretical formula list so that they could also be assigned (Supporting Information Table S3).

The tolerance allowed for formula assignment was set to 5 ppm ($1 \times 10^6 \times \Delta m/m$). Because this mass window was not always sufficiently small to have one unambiguous formula in the theoretical list, and with the knowledge that all possible formulas were not present in the list, an isotope ratio confirmation was also conducted for every formula assignment (Stoll et al. 2006). For each detected signal, the corresponding ^{13}C peak at $m/z + 1.00335 \pm 2$ ppm was determined, and the intensity ratio (R_i) of the two peaks was compared to the

theoretical value (P) given that carbon is 1.1% ^{13}C , as $P = n \cdot 1.1/98.9$, where n is the number of carbon atoms. When two potential formulas occurred within 5 ppm, the formula with the closest observed intensity ratio R_i to P was selected. If R_i was identical for the two options, the closest mass accuracy formula was selected. In all cases, the R_i was divided by P to give an assignment confidence metric, and formulas were considered as “confidently assigned” if R_i/P was 0.8–1.2.

All assignments were collected as a single matrix for each sample, with rows according to formulas in the theoretical list, columns as retention times (transients) and matrix values as assigned intensities. Corresponding matrices of the same dimensions were also prepared for the assignment mass error, assignment confidence metric, and number of candidate formulas that were considered.

Chromatographic peaks were identified among the assigned mass channels by using the *findpeaks* algorithm in Matlab. Settings for the tolerances of this algorithm (Supporting Information Table S4) were tuned according to the behavior of the compounds in the standard mixture. Chromatographic peak signals were aligned between samples using a clustering algorithm (*subclust*, Matlab). Peaks were retained in the data set only if the settings were satisfied.

The full data processing pipeline led to two matrices for each sample. The first contained all reliable signals (above noise), which were assigned to formulas—this pipeline is similar to our usual processing of complex DOM samples (Hawkes et al. 2018, 2019; Patriarca et al. 2018). The second contained peak heights that were determined by the *findpeaks* algorithm and matched between samples with the *subclust* algorithm. Here, a single value (the peak prominence) was given for each sample in columns, and rows were designated to the formula and retention time average of that clustered peak. Peak intensities were changed to zero if they were less than $3\times$ the average intensity of the same peak in the blank triplicates.

The polarity of peaks (octanol/water partitioning coefficient, $\log P$) was estimated by calibration of the reversed phase separation retention time of a series of 16 compounds purchased from Sigma Aldrich (Supporting Information Table S5 and Figure S1), and use of the ChemAxon estimated $\log P$ values from PubChem.

In this study, we reserve the term “peak” for well-resolved chromatographic peaks and refer to m/z peaks as signals. Confidently assigned peaks means chromatographic peaks that had an isotopic signature closely matching that expected by the formula.

Results

Cyanobacterial growth and organic material released in the tested treatments

The growth of *M. aeruginosa* was consistently higher in the artificial treatment (BG11₀ medium) compared to the natural treatment (filtered lake Erken water; Fig. 1).

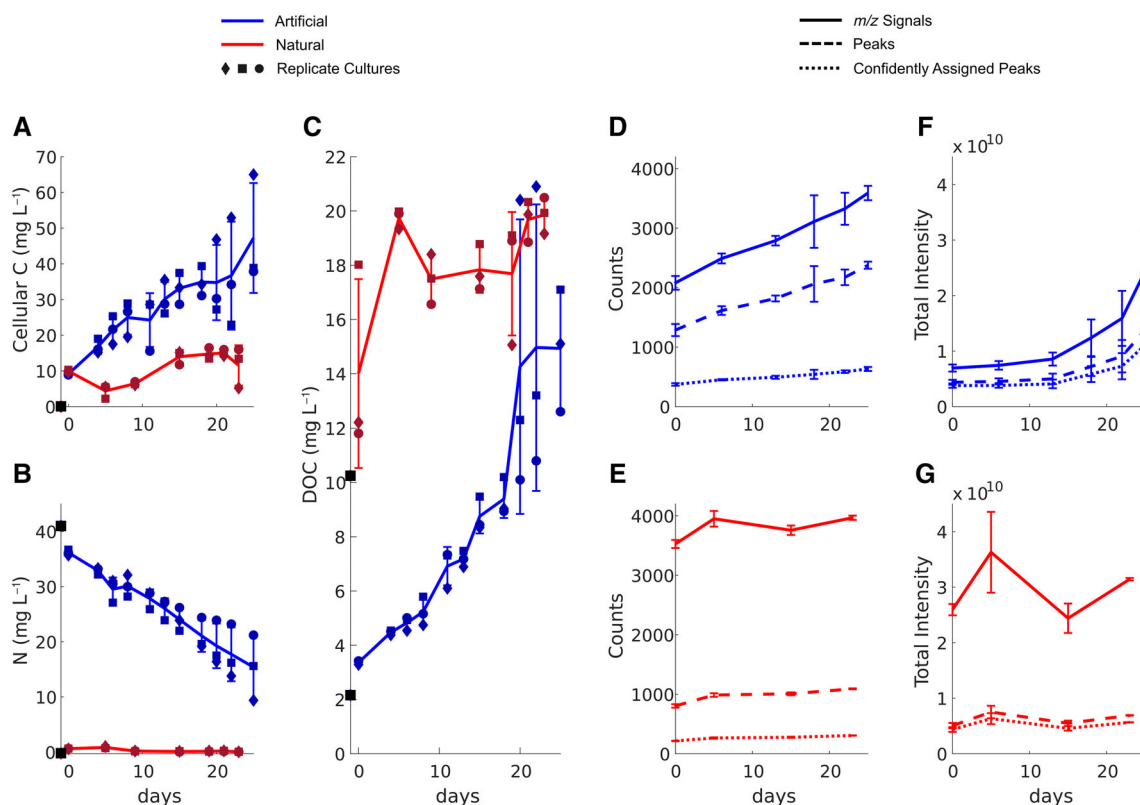


Fig 1. Incubations of *M. aeruginosa* in artificial (blue) and natural (red) media. Error bars indicate standard deviation of three replicate cultures (diamond, square, and circle markers; for simplicity reported only in **A–C**). **(A)** The cellular carbon (mg L⁻¹); **(B)** The total dissolved nitrogen (mg L⁻¹); **(C)** DOC (mg L⁻¹); the black squares on the y-axis of panels **(A–C)** show the concentrations of the media prior to inoculation; **(D, E)** The number of assigned signals and peaks; **(F, G)** The total summed intensity of the assigned signals and peaks. See data in Supporting Information Table S2.

Biomass (Fig. 1A) increased steadily in the *artificial* treatment and was consistent with the production of dissolved organic material as shown by the DOC concentrations (Fig. 1C). Conversely, in the *natural* treatment, there was a loss of biomass the first week accompanied by an increase in the DOC levels from ~14 mg L⁻¹ at the beginning of the experiment to ~20 mg L⁻¹ at the end of the first week.

There was a clear difference in DOC concentration between the two treatments from the beginning of the experiment (Fig. 1C). This is attributed to the existing DOM present in Lake Erken water (~10 mg L⁻¹). During the cyanobacteria incubation, the *artificial* treatment (blue lines) showed a rapid and consistent growth, almost doubling the amount of organic material within the first 10 d of incubation (about 320 ppb of DOC d⁻¹) and achieving a total of four times the initial DOC concentration by the end of the experiment. For the *natural* treatment (red lines), cyanobacterial growth rate was different; despite an initial rapid increase, the amount of DOC stabilized after 7 d. The *artificial* treatment produced about twice as much DOC during the experiment (12 vs. 6 mg L⁻¹), and had approximately ~5× more cyanobacterial cellular carbon by the end. Notably, despite the small pore size used for the filtration, not all heterotrophic bacteria were

removed from the *natural* treatment, enabling some regrowth (Supporting Information Figure S2).

DOC data were compared to the results obtained by mass spectrometry analysis (Fig. 1D–G). The different traces display assigned *m/z* signals (solid lines), observed peaks (dashed lines), and confidently assigned peaks (dotted lines), the latter resulting from the restrictions imposed by the isotopic pattern confirmation (Stoll et al. 2006). The absolute number of *m/z* signals, observed peaks (Fig. 1D,E), and their associated intensities (Fig. 1F,G) over the incubation period mirrored the trend in DOC values for the *artificial* treatment, while in the *natural* treatment the signals were almost stable despite an increase in DOC. The cyanobacteria in the *artificial* medium constantly enriched the culturing environment with new ionizable material, as confirmed by the continuous increase in the number of assigned *m/z* signals, peaks and their overall intensity (Fig. 1D,F, blue traces). Contrarily, no similar dynamic was observed for the *natural* cultures, instead there was overall stability of assigned *m/z* signals, peaks and associated intensities (Fig. 1E,G, red traces).

The relative standard deviation (RSD) among the three replicate cultures was consistently below 15% throughout the incubation period for both incubations, except a deviation

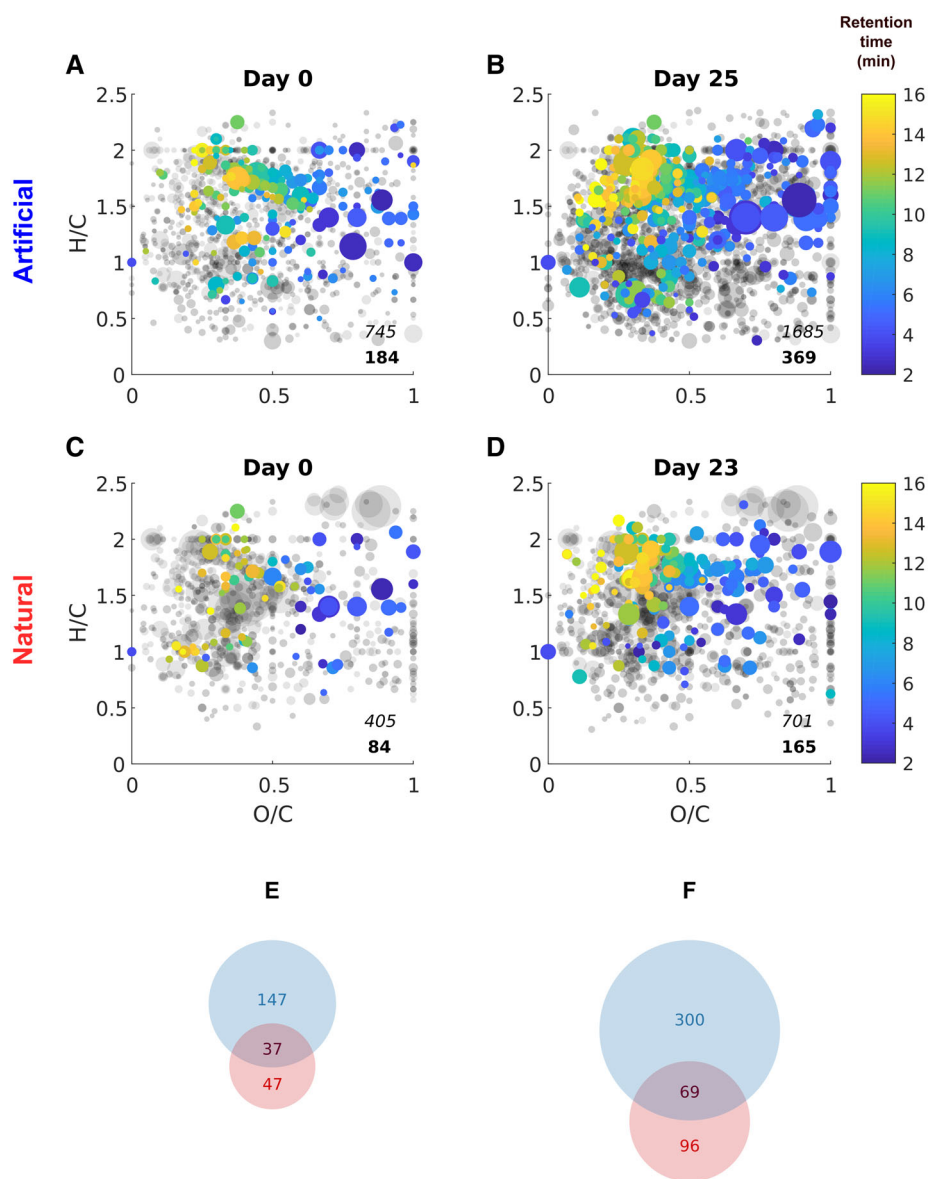


Fig 2. (A–D) Chromatographic peak distribution observed in the initial (left) and final (right) stages of the cyanobacteria incubation. Van Krevelen diagrams for the *artificial* (A, B) and *natural* (C, D) treatments in replicate 1 in each case. These plots show the molecular distribution of the chromatographic peaks in relation to the H/C and O/C atomic ratios of the assigned monoisotopic formula; the size of each point reflects the peak intensity and the color scheme correlates to the chromatographic elution time (in minutes). The faded gray points are all observed peaks with putative, nonconfident formula assignments as opposed to the colored points, which indicate the confidently assigned peaks. In the lower right corner of each diagram, the number of observed (*italic*) and confidently assigned (*bold*) peaks is reported. (E, F) Venn diagrams show the number of confidently assigned peaks for the *artificial* (blue) and *natural* (red) treatments in the initial (E) and final (F) stages of incubation. The overlapping areas identify peaks common for both treatments with respect to molecular formula and retention time.

observed toward the end of the growth curve in the *artificial* incubation (RSD ~ 40%) as well as a sudden shift on the first incubation day of the *natural* treatment (RSD ~ 24%). However, all replicate cultures showed similar trends (Fig. 1, error bars), thus confirming the experimental reproducibility.

The number and intensity of chromatographic peaks increased during the incubation, particularly in the artificial treatment (Fig. 2). At the beginning of each treatment

(Fig. 2A,C,E), only a few chromatographic peaks were observed. Already in the early phase of the incubation, a difference was visible, as seen in the Venn diagram (panel E) with a minority of common peaks between the *artificial* and *natural* incubations. The results point to a substantial increase in the production and release of new material by the end of the incubation period (Fig. 2B,D,F), especially for the *artificial* treatment. The Venn diagram (Fig. 2F) highlights that many

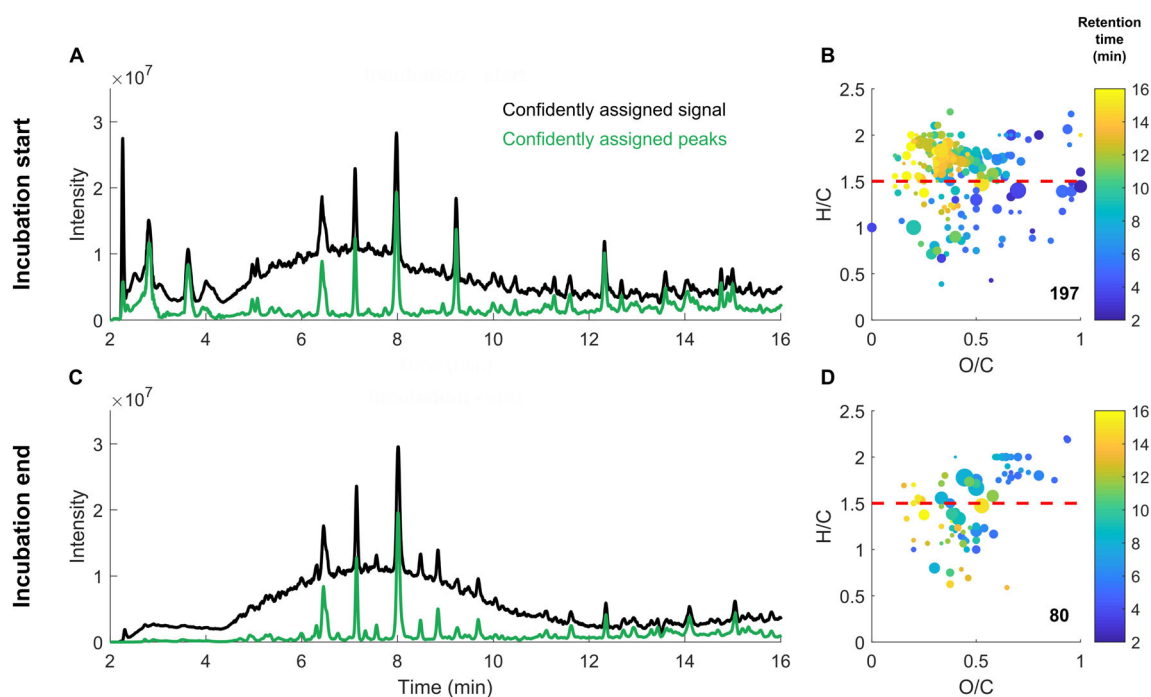


Fig 3. Start (day 0) and end (day 14) profiles of the cyanobacteria-derived DOM incubated with unfiltered Lake Erken water. Only confidently assigned data are considered. **(A, C)** Chromatographic profiles of: all m/z signals (black); peak-associated signal (green). **(B, D)** van Krevelen diagrams showing the molecular distribution of the confidently assigned peaks, together with their intensity (point size) and elution time in minutes (color). The red dashed line ($H/C > 1.5$) identifies the H/C ratio above which analytes have previously been annotated as labile (D'Andrilli et al. 2015). The number of peaks observed at each incubation stage is reported in the bottom right corner of each diagram.

more peaks were detected in the *artificial* treatment compared with the *natural* incubation. Additionally, only a small fraction of the observed chromatographic peaks were common to both experiments, most peaks being unique to each treatment.

The van Krevelen diagrams (Fig. 2A–D) display the chemical composition of the ionizable DOM detected in the two treatments. At the end of the incubation, a wide range of compound types were found, covering much of the van Krevelen space, but specific regions of the van Krevelen diagram were more densely populated, in particular the aliphatic area ($H/C > 1.5$). The *artificial* treatment was richer in material, characterized by thousands of chromatographic peaks that covered an extensive portion of the van Krevelen diagram associated to a large range of polarities (retention times 2–16 min, Fig. 2B). In comparison, the *natural* treatment had lower peak abundance with slightly less coverage in van Krevelen space.

Cyanobacteria-derived DOM fate in natural waters

The ability of heterotrophic bacteria to efficiently remove the cyanobacteria-derived DOM was assessed in an additional experiment. When concentrated cyanobacteria-derived DOM from the *artificial* treatment was incubated with unfiltered lake water (Erken), a change in the composition of the added organic material was observed (Fig. 3), including complete

removal of 53% of all detected peaks from the starting point after 48 h. By the end of the experiment, 69% of the initially detected peaks were removed.

The difference between the initial and final stages of the *lability test* profiles can be attributed to background DOM in Lake Erken that does not elute as resolved chromatographic peaks (Fig. 3). Few changes were observed in the overall assigned intensity (black profiles) of the *lability test* from start to end, but clear differences emerged from the comparison of the chromatographically resolved material (green profiles). In fact, the hydrophilic material (elution time < 5 min) and the more hydrophobic species (elution time > 8.5 min) decreased dramatically over the incubation period. In contrast, medium polarity material (elution time between 5 and 8.5 min) was more resistant to removal, and in some cases, may have been produced—although further experimentation is required to confidently demonstrate this. The contrast between the initial and final stages of the incubation is more evident in the van Krevelen diagrams (Fig. 3B,D) where the confidently assigned chromatographic peaks are displayed, based on their molecular distribution, intensity, and elution time. As previously observed, the beginning of the incubation was characterized by a high abundance in hydrophilic and hydrophobic species, preferentially removed below the detection limit during the incubation. In particular, the depletion of the species located in

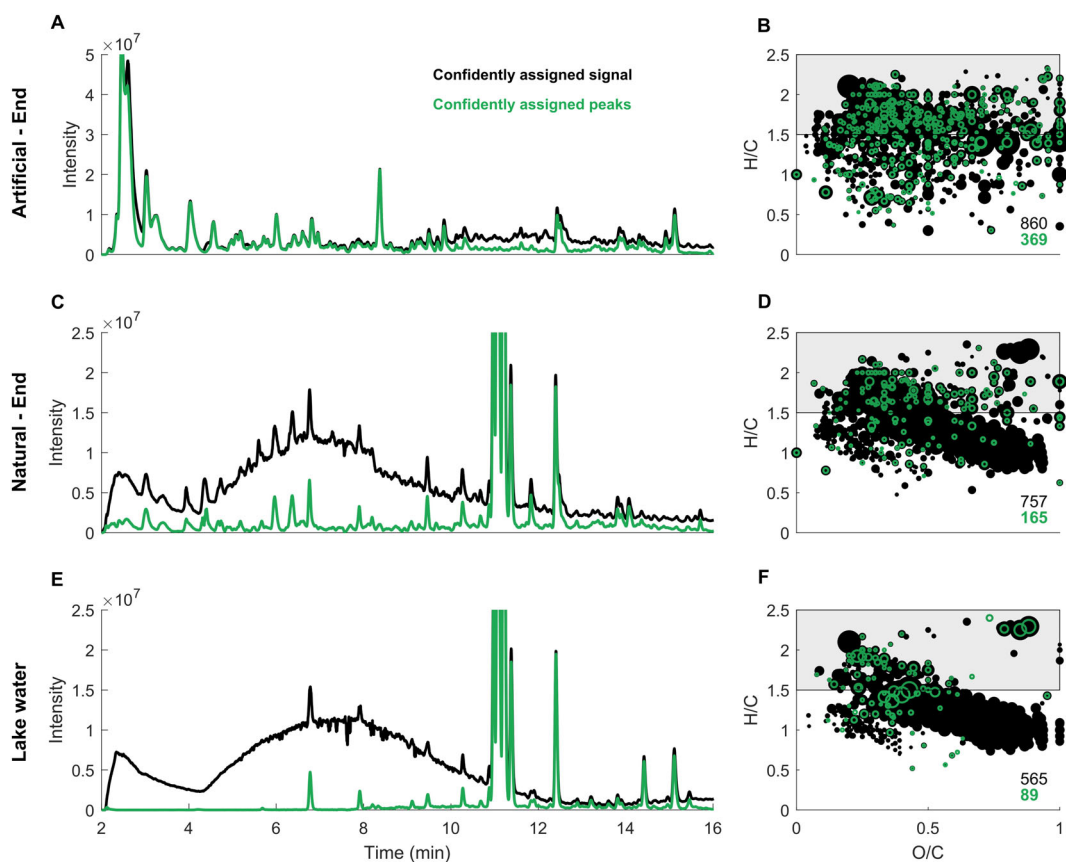


Fig 4. Cyanobacteria-derived DOM observed in the *artificial* (A, B) and *natural* (C, D) treatments and organic material from Lake Erken (E, F). Only confidently assigned data are considered. (A, C, E) Chromatographic profiles of: m/z signals (black) and peak-associated signal (green), note the different y-axis scale in (A). (B, D, F) van Krevelen diagrams showing the molecular distribution of m/z signals (black points) and peaks (green outline), together with their intensity (point size). The number of m/z signals and peaks is reported in the lower right corner of each diagram. The shaded areas identify the region previously identified as labile ($H/C > 1.5$).

the aliphatic region ($H/C > 1.5$; above red dashed line) could be observed. Data analysis revealed that while 508 peaks observed on day 0 were not detected at the end

of the incubation (day 14; 80% of the chromatographically resolved peaks), only six new chromatographic features emerged.

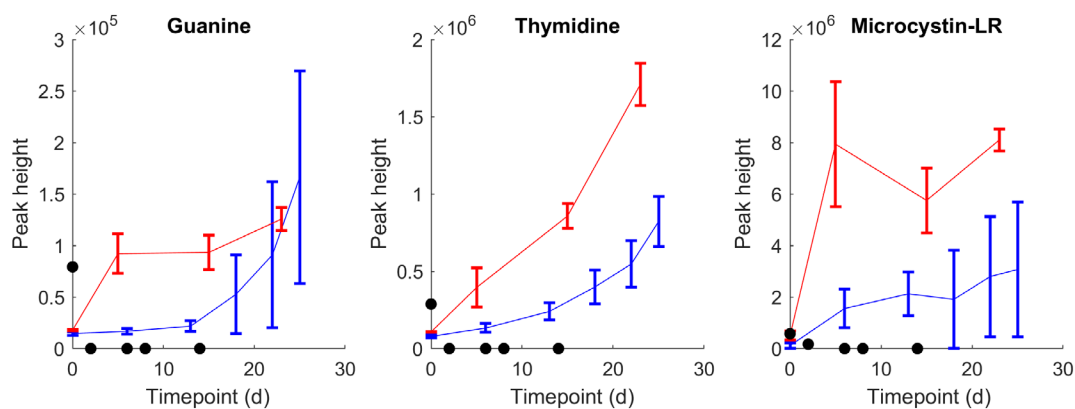


Fig 5. Three selected peaks with putative identifications. The *artificial* treatment (blue) *natural* treatment (red) and *incubation* experiment (black points) are shown overlaid. The error bars (available only for the *artificial* and *natural* treatments) indicate the variation (standard deviation) among the three replicates.

Cyanobacteria-derived DOM vs. natural water DOM

There was a substantial difference among the organic material derived from the *artificial* and *natural* treatments (Fig. 4A–D) and the DOM observed in the lake water (Lake Erken; Fig. 4E,F).

The DOM released by the primary producer *M. aeruginosa* during the artificial treatment generated a feature-rich chromatogram in which a large portion of the total assigned intensity was attributed to chromatographically resolved peaks (Fig. 4A; black and green traces), and almost half of the assigned m/z signals corresponded to a singly eluting compound. This observation can be clearly made also from the van Krevelen diagrams (Fig. 4B), where the green marks identify the chromatographic peaks, which represent a substantial percentage (43%) of the overall number of assigned peaks. Substantially less chromatographic features were found in the cyanobacteria-DOM released in the *natural* treatment. The broad molecular complexity deriving from the culturing medium reduced the abundance of resolved material (Fig. 4C). Despite the suppression, an important number of peaks could be detected and a large percentage (22%) of the assigned signals was translated into chromatographic profiles (Fig. 4D). For both treatments, a substantial portion of the eluting material is densely distributed in the aliphatic area ($H/C > 1.5$, shaded area), which has previously been characterized as labile (D'Andrilli et al. 2015).

Lake Erken had a completely different profile, showing only a remote correlation between the assigned signals and the chromatographic peaks (Fig. 4E) and demonstrating that the isomeric complexity of the lake derived DOM prevents the isolation of singly eluting compounds (at least for the current chromatographic settings). This leads to a vast amount of assigned m/z signals which cannot be translated to individually eluting components. This observation can be better appreciated in the associated van Krevelen diagram (Fig. 4F), where a limited number of chromatographic peaks could be observed (16%) and modest peak abundance was registered in the aliphatic or labile region. Several large peaks eluting close to 11 min were observed in Lake Erken water (also visible in the *natural* treatment) for this sampling occasion (02 April 2019). It is unclear whether these were genuinely present in the lake or introduced during the sampling or filtering process, but they were not found on the later sampling occasion (11 September 2019; Fig. 3).

Targeted metabolites

A list of 182 known metabolites was included in the theoretical formula list for m/z signal assignment, and 78 of these were matched to a mass in the *artificial* or *natural* treatment datasets. A further check used the empirically estimated $\log P$ (octanol/water partitioning constant) of the observed peaks and compared the calculated $\log P$ values of the metabolites. If the calculated $\log P$ was within the standard error (0.5 units, 95% confidence interval) of the

empirically estimated $\log P$, then the metabolite was considered putatively assigned (see Supporting Information). Nineteen peaks were given putative metabolite assignments, including Guanine, Thymidine, and Microcystin-LR, which were found in all three datasets (*natural*, *artificial*, and *lability test*) and all increased in concentration during the incubations (Fig. 5). The nucleotides were removed in less than 2 d in the *lability test*, while the toxin was removed slightly slower and was not detectable after 5 d.

Discussion

Our study showed that axenic cultures of cyanobacteria produce a broad range of compounds in terms of chemical properties, including polarity and saturation. We also found evidence that these molecules are quickly removed in the presence of heterotrophic bacteria, explaining why they are typically not seen in aquatic samples, even when cyanobacteria are present in abundance.

Sample coverage by the UPLC-HRMS technique

The “analytical window” employed in any study is of critical importance to the results obtained, and our obtained signals do not necessarily correspond to fluorescence indices for autochthonous DOM (McKnight et al. 2001). The ionizable cyanobacteria-derived DOM portion is likely to represent a minority of total cyanobacteria DOM (Mykkestad 2005), as indicated particularly clearly in the *natural* treatment, in which a large increase in DOC did not correspond to a significant change in assigned signals over the DOM background (Fig. 1), which was rich in the ubiquitous carboxylic acids (Witt et al. 2009; Zark et al. 2017; Fig. 4). However, the material measured (particularly the well-resolved chromatographic peaks) is likely to be of key importance to the microbial food web and for other biogeochemical processes. This biogeochemical importance is expected due to the relative high concentration needed for detection (compared to individual analytes in DOM; Zark et al. 2017) and in some cases, known biological utility of the molecules (e.g., Thymidine; Fig. 5).

Our study investigates material that passes through a filter, is sufficiently nonvolatile to remain after vacuum centrifugation, retains on a reverse phase column material at acidic pH, ionizes in electrospray (negative mode), and can be attributed a singly charged formula. This does not include polysaccharides and proteins, which have previously been characterized in extracellular mixtures from cyanobacteria, including *M. aeruginosa* (Mykkestad 2005; Pivokonsky et al. 2014). Instead, our study focuses on the ionizable metabolite portion (Bittar et al. 2015a; Bai et al. 2017; Powers et al. 2019), with a view to assessing the importance of this autochthonous material in studies that use a similar analytical pipeline to characterize freshwater DOM.

What ionizable DOM does cyanobacteria produce (cyanobacteria-derived DOM) in the artificial (axenic) environment?

The growth rate of cyanobacteria in axenic conditions (*artificial* treatment) was rapid and continuous over the incubation period, as highlighted by the cellular biomass levels and DOC concentrations (Fig. 1A,C—blue profile). At the moment of inoculation, an immediate release of fresh organic material in solution was registered, followed by a constant increase in cyanobacteria-derived DOM concentration due to the production and accumulation of fresh organic material in the medium. The UPLC-HRMS data obtained from the ionizable material reflects the same trend (Fig. 1D,F). The absolute number of m/z signals highlights the production and the increasing complexity of the organic mixture, while the rise of chromatographic peaks confirmed the accumulation of resolvable metabolites to a level able to satisfy the restriction for peak identification. Numerous known metabolites were detected and putatively identified based on their mass and polarity (Supporting Information Table S3), but our study was not designed as a targeted analysis, and instead we attempted a nontargeted approach in line with the DOM biogeochemistry literature. The other chromatographically resolved peaks are also likely to be truly endogenous compounds but were not targeted for identification here.

Despite the increasing complexity over the incubation period, more than 50% of the assigned m/z signals were recognized as chromatographic peaks, meaning that a large part of the produced material could be observed and possibly isolated as singly eluting species. An analogous tendency is displayed by the intensity levels (Fig. 1F). About 50% of the overall assigned intensity was derived exclusively from the chromatographic peaks while the rest of the signal can be attributed to unresolved peaks or low abundance material unable to pass the set threshold for peak recognition. The total intensity associated with the m/z signals was expected to coincide with the resolved peak intensity toward the end of the incubation due to the cyanobacteria-derived DOM accumulation, but interestingly the gap between resolved and nonresolved intensity remained almost unaltered throughout the incubation. This suggests that both chromatographic peaks and unresolved or low abundance material experienced a similar increment, thus maintaining the same intensity ratio over the incubation time. Despite the ability of the method to observe a large number of chromatographic peaks, a major reduction of the data set was imposed by the necessity to confidently assign formulas via isotope ion pattern to the observed signals. About 26–29% of the chromatographic peaks were “confidently assigned” and despite the use of this conservative approach, it is evident that they account for the majority of intensity (Fig. 1F, dotted profile).

The van Krevelen diagrams in Fig. 2A,B offer an insight into the chemical composition of the cyanobacteria derived material in the artificial treatment over the incubation period.

Cyanobacteria-derived DOM released in axenic conditions showed a large variety of polarities, particularly rich in hydrophilic components and aliphatic material ($H/C > 1.5$), similar to previous results with direct infusion ESI-HRMS (Bittar et al. 2015a; Gonsior et al. 2019). By the end of the incubation, more than 56% of the confidently assigned peaks were found in the aliphatic (labile) region, suggesting that this material ought to be easily removed by heterotrophs (Bittar et al. 2015b; D’Andrilli et al. 2015).

Organic material continuously eluted from the column between 2 and almost 17 min. This is equivalent to a broad octanol/water partitioning constant ($\log P$) range of approximately -3 to 5 , according to the retention time of mannitol (2.0 min, $\log P \sim -3.1$) and fusidic acid (17.7 min, $\log P \sim 5.5$) by the same method (Supporting Information Figure S1). The initial part of the chromatogram was diverted to waste to avoid interferences with the MS, but it is plausible that more hydrophilic ionizable material was present, along with the hydrophilic polysaccharides and proteins that are not detected by this method (Pivokonsky et al. 2014).

This chemical profile of a large polarity range of mainly aliphatic material is highly different from the typical DOM found in freshwater, which has polarities restricted to about $\log P$ 0–3 (Namjesnik-Dejanovic and Cabaniss 2004) and usually occupies a central region of the van Krevelen diagram between H/C 0.7–1.5 (Fig. 4) (D’Andrilli et al. 2015). This clear compositional difference between observed natural mixtures of ionizable DOM and cyanobacteria-derived DOM from *M. aeruginosa* has two likely and nonconflicting explanations: (1) *M. aeruginosa* produces low quantities of ionizable DOM in the environment compared to the flux of terrestrial carboxylic acids from soils; (2) the cyanobacteria-derived DOM is very labile, so when produced it is quickly consumed, and to some extent also transformed into compounds more similar to DOM (Lechtenfeld et al. 2015).

Cyanobacteria-derived DOM in the natural environment

We conducted two further experiments that allowed us to explore the lability of cyanobacteria-derived DOM in the natural environment, thereby exploring the consumption theory above. First, a second growth experiment was undertaken with filtered water from a low nitrate lake (Erken, Sweden), in which heterotrophic bacteria were (involuntarily) cocultivated with *M. aeruginosa* (named the *natural* treatment). Second, we conducted an incubation of unfiltered water from the same lake with concentrated cyanobacteria-derived DOM (*lability test*).

In contrast to the *artificial* treatment, characterized by steady axenic cyanobacteria growth and DOM release (Fig. 1), a more complex profile emerged from the *natural* incubation, as seen in the halted accumulation of cellular biomass and the DOC concentrations after the initial growth phase. In the *natural* treatment, a lower number of chromatographically resolved features were produced (706 ± 8 vs. 1717 ± 39). This

indicates that either the cyanobacteria-derived DOM was consumed by heterotrophic bacteria or that *M. aeruginosa* did not release cyanobacteria-derived DOM under the prevailing growth conditions, possibly in response to the presence of other bacteria or nutrient limitation (Huang et al. 2012; Zhao et al. 2019). A third explanation could be that the cyanobacteria-derived DOM signal was suppressed by background DOM.

In the *lability test* experiment, we found that heterotrophs could indeed consume the majority of ionizable cyanobacteria-derived DOM within less than 2 d. Most of the peaks removed by bacterial degradation were located in the labile region of the van Krevelen diagram, confirming the fast turnover of the aliphatic material (D'Andrilli et al. 2015). Contrarily to Bai et al. 2017, saturated compounds were preferentially transformed and removed below the detection limit for peak identification along with the most hydrophilic and hydrophobic species, as shown in Fig. 3.

Interestingly, the abundant hydrophilic peaks and majority of hydrophobic peaks were preferentially removed in this experiment, leaving the resulting chromatographic profile at a narrower middle range with less chromatographic features, more similar to the background DOM which is relatively stable in the lake. The consumption of cyanobacteria-derived DOM by heterotrophic bacteria is consistent with previous studies that have reported high bacterial growth efficiency and production on algal lysates as a carbon source (Bertilsson and Jones 2003; Pérez and Sommaruga 2006; Attermeyer et al. 2014). The results also corresponds well with studies that use carbon isotope ratios to monitor preferential removal of autochthonous DOM in freshwater lakes (Maki et al. 2010).

Although some chromatographically resolved peaks were produced in the *lability test* experiment, they were few in number and the majority of signal loss did not seem to be recovered as transformation products. This indicates that material was lost from the dissolved phase due to respiration or use in cell growth, or was transformed to compounds that do not ionize by electrospray.

The numbers of peaks visible at the beginning of the *lability test* experiment (197; Fig. 3) were fewer than those previously visualized at the end of the artificial incubation (369; Fig. 2). While the cyanobacteria-derived DOM concentration was slightly lower (cf. 10 ppm vs. 15 ppm), this difference is probably more related to the masking or suppression effect of the lake-DOM material. Fewer hydrophilic and mid polarity species were detected by the method. However, despite the increased mixture complexity, the main species characterizing the cyanobacteria-derived DOM profile were still able to satisfy the threshold for peak recognition and assignment confidence and similar to the axenic culture, the majority of the peaks (64%) populated the “labile” or “aliphatic” region of the van Krevelen diagram. This particular analytical problem poses a challenge in future work, as the suppression effect can easily

be interpreted as a lack of cyanobacteria-derived DOM occurrence in a sample, particularly if direct infusion ESI-HRMS is employed rather than chromatographic separation (Patriarca et al. 2018). Different ionization techniques or more targeted sample preparation toward the aliphatic fraction may be useful when analysis of autochthonous DOM is required in aquatic samples. Problematically, the “aliphatic” fraction covers a very wide polarity range, so typical extraction techniques such as solid phase extraction on C18 or Agilent PPL are unlikely to be useful. Low oxygen aliphatics are also more likely to have higher volatility, and this may also restrict sample recovery by some methods.

What happens to cyanobacteria-derived DOM when it is consumed by heterotrophs?

Differences between the *artificial* and *natural* treatment incubations were expected; however, the cyanobacterial growth in the *natural* incubation displayed a surprising trend. A rapid increase in DOC concentration was observed in the first week of incubation during a period with a slight decrease in $>0.7 \mu\text{m}$ cellular biomass associated with *M. aeruginosa* (Fig. 1, day 5). Corresponding to this event, a substantial increase in the total intensity of the assigned signals was observed, including the toxin microcystin-LR (Fig. 5). This event may suggest a release of intracellular material in the medium (Bittar et al. 2015b) and potentially also some degree of antagonism between *M. aeruginosa* and competing heterotrophic bacteria. This overall increase in DOC was not fully mirrored in the intensity of ionizable carbon or intensity associated to chromatographic peaks, and may have been constituted by the more traditionally characterized polysaccharide and protein material (Pivokonsky et al. 2014).

It is possible that autotrophic DOM such as cyanobacteria-derived DOM is gradually processed by heterotrophic microbial food webs (Sarmiento and Gasol 2012; Teeling et al. 2012) so that increasingly recalcitrant and diverse DOM is produced, a topic of debate in marine systems (Lechtenfeld et al. 2015; Osterholz et al. 2015; Mentges et al. 2019). In our data, this would be manifested by an increase in broad signals that do not resolve into chromatographic peaks during consumption of cyanobacteria-derived DOM, such as during the *lability test* experiment. There was no clear evidence for this phenomenon in our data, but difficulties with quantification of mass spectrometry signals may have hampered our efforts in observing this effect. An alternative fate of cyanobacteria-derived DOM is mineralization to CO_2 and incorporation into heterotrophic cellular matter. While some methodological difficulties still remain with respect to determining the eventual fate of autotrophic cyanobacteria-derived DOM in lake environments, we found clear evidence that the primary metabolites produced by *M. aeruginosa* are not resistant to biological consumption when in the presence of in typical lake bacterioplankton communities.

Conclusions

The cyanobacterium *M. aeruginosa* produces aliphatic ionizable DOM (cyanobacteria-derived DOM). During axenic growth of this species, high diversity and abundance of compounds with high (> 1.5) H to C ratios was detected. These compounds appeared to be labile, being less prevalent in presence of freshwater heterotrophic bacteria.

Approximately half of the ionizable cyanobacteria-derived DOM was attributable to well-resolved chromatographic peaks indicative of freshly produced metabolites, including some putatively identified compounds such as nucleotides and a toxin. This feature richness was specific to the cyanobacteria incubations and was clearly different from the highly degraded, broad features typically found in freshwater DOM.

Cocultures of *M. aeruginosa* or incubation of heterotrophic bacteria from lake water in cyanobacteria-derived DOM revealed a high biological lability, and demonstrated that ionizable cyanobacteria-derived DOM was rapidly processed in natural settings to leave samples containing the more typically observed, poorly resolvable DOM.

References

- Aluwihare, L. I., D. J. Repeta, and R. F. Chen. 1997. A major biopolymeric component to dissolved organic carbon in surface sea water. *Nature* **387**: 166–169. doi:10.1038/387166a0
- Amon, R. M. W., and R. Benner. 1996. Bacterial utilization of different size classes of dissolved organic matter. *Limnol. Oceanogr.* **41**: 41–51. doi:10.4319/lo.1996.41.1.0041
- Attermeyer, K., T. Hornick, Z. E. Kayler, A. Bahr, E. Zwirnmann, H. P. Grossart, and K. Premke. 2014. Enhanced bacterial decomposition with increasing addition of autochthonous to allochthonous carbon without any effect on bacterial community composition. *Biogeosciences* **11**: 1479–1489. doi:10.5194/bg-11-1479-2014
- Bai, L., C. Cao, C. Wang, H. Xu, H. Zhang, V. I. Slaveykova, and H. Jiang. 2017. Toward quantitative understanding of the bioavailability of dissolved organic matter in freshwater lake during cyanobacteria blooming. *Environ. Sci. Technol.* **51**: 6018–6026. doi:10.1021/acs.est.7b00826
- Bertilsson, S., and J. B. Jones. 2003. Supply of dissolved organic matter to aquatic ecosystems: Autochthonous sources, In S. E. G. Findlay, and R. L. Sinsabaugh, (Eds.) p. 3–19. *In* Aquatic ecosystems. USA: Elsevier Science.
- Bittar, T. B., A. Stubbins, A. A. H. Vieira, and K. Mopper. 2015a. Characterization and photodegradation of dissolved organic matter (DOM) from a tropical lake and its dominant primary producer, the cyanobacteria *Microcystis aeruginosa*. *Mar. Chem.* **177**: 205–217. doi:10.1016/j.marchem.2015.06.016
- Bittar, T. B., A. A. H. Vieira, A. Stubbins, and K. Mopper. 2015b. Competition between photochemical and biological degradation of dissolved organic matter from the cyanobacteria *Microcystis aeruginosa*. *Limnol. Oceanogr.* **60**: 1172–1194. doi:10.1002/lno.10090
- Cortés-Francisco, N., and J. Caixach. 2013. Molecular characterization of dissolved organic matter through a desalination process by high resolution mass spectrometry. *Environ. Sci. Technol.* **47**: 9619–9627. doi:10.1021/es4000388
- D'Andrilli, J., W. T. Cooper, C. M. Foreman, and A. G. Marshall. 2015. An ultrahigh-resolution mass spectrometry index to estimate natural organic matter lability. *Rapid Commun. Mass Spectrom.* **29**: 2385–2401. doi:10.1002/rcm.7400
- Gonsior, M., L. C. Powers, E. Williams, A. Place, F. Chen, A. Ruf, N. Hertkorn, and P. Schmitt-kopplin. 2019. The chemodiversity of algal dissolved organic matter from lysed *Microcystis aeruginosa* cells and its ability to form disinfection by-products during chlorination. *Water Res.* **155**: 300–309. doi:10.1016/j.watres.2019.02.030
- Hawkes, J. A., C. T. Hansen, T. Goldhammer, W. Bach, and T. Dittmar. 2016. Molecular alteration of marine dissolved organic matter under experimental hydrothermal conditions. *Geochim. Cosmochim. Acta* **175**: 68–85. doi:10.1016/j.gca.2015.11.025
- Hawkes, J. A., N. Radoman, J. Bergquist, M. B. Wallin, L. J. Tranvik, and S. Löfgren. 2018. Regional diversity of complex dissolved organic matter across forested hemiboreal headwater streams. *Sci. Rep.* **8**: 16060. doi:10.1038/s41598-018-34272-3
- Hawkes, J. A., P. J. R. R. Sjöberg, J. Bergquist, and L. J. Tranvik. 2019. Complexity of dissolved organic matter in the molecular size dimension: Insights from coupled size exclusion chromatography electrospray ionisation mass spectrometry. *Faraday Discuss.* **218**: 52–71. doi:10.1039/c8fd00222c
- Hertkorn, N., M. Frommberger, M. Witt, B. P. Koch, P. Schmitt-kopplin, and E. M. Perdue. 2008. Natural organic matter and the event horizon of mass spectrometry. *Anal. Chem.* **80**: 8908–8919. doi:10.1021/ac800464g
- Huang, W., H. Chu, and B. Dong. 2012. Characteristics of algogenic organic matter generated under different nutrient conditions and subsequent impact on microfiltration membrane fouling. *Desalination* **293**: 104–111. doi:10.1016/j.desal.2012.03.001
- Koch, B. P., K. U. Ludwichowski, G. Kattner, T. Dittmar, and M. Witt. 2008. Advanced characterization of marine dissolved organic matter by combining reversed-phase liquid chromatography and FT-ICR-MS. *Mar. Chem.* **111**: 233–241. doi:10.1016/j.marchem.2008.05.008
- Koehler, B., E. Von Wachenfeldt, D. Kothawala, and L. J. Tranvik. 2012. Reactivity continuum of dissolved organic carbon decomposition in lake water. *J. Geophys. Res. Biogeosci.* **117**: 1–14. doi:10.1029/2011JG001793
- Kothawala, D. N., E. von Wachenfeldt, B. Koehler, and L. J. Tranvik. 2012. Selective loss and preservation of lake water

- dissolved organic matter fluorescence during long-term dark incubations. *Sci. Total Environ.* **433**: 238–246. doi:10.1016/j.scitotenv.2012.06.029
- Lechtenfeld, O. J., N. Hertkorn, Y. Shen, M. Witt, and R. Benner. 2015. Marine sequestration of carbon in bacterial metabolites. *Nat. Commun.* **6**: 1–8. doi:10.1038/ncomms7711
- Maki, K., C. Kim, C. Yoshimizu, I. Tayasu, T. Miyajima, and T. Nagata. 2010. Autochthonous origin of semi-labile dissolved organic carbon in a large monomictic lake (Lake Biwa): Carbon stable isotopic evidence. *Limnology* **11**: 143–153. doi:10.1007/s10201-009-0299-z
- McKnight, D. M., E. W. Boyer, P. K. Westerhoff, P. T. Doran, T. Kulbe, and D. T. Andersen. 2001. Spectrofluorometric characterization of dissolved organic matter for indication of precursor organic material and aromaticity. *Limnol. Oceanogr.* **46**: 38–48. doi:10.4319/lo.2001.46.1.0038
- Mentges, A., C. Feenders, C. Deutsch, B. Blasius, and T. Dittmar. 2019. Long-term stability of marine dissolved organic carbon emerges from a neutral network of compounds and microbes. *Sci. Rep.* **9**: 1–13. doi:10.1038/s41598-019-54290-z
- Myklestad, S. M. 2005. Dissolved organic carbon from phytoplankton. *Mar. Chem.* **5**: 111–148. doi:10.1007/10683826_5
- Namjesnik-Dejanovic, K., and S. E. Cabaniss. 2004. Reverse-phase HPLC method for measuring polarity distributions of natural organic matter. *Environ. Sci. Technol.* **38**: 1108–1114. doi:10.1021/es0344157
- Oliver, R. L., and G. G. Ganf. 2000. Freshwater blooms. In *The ecology of cyanobacteria*. In B. Whitton, and M. Potts, (Eds.) The Netherlands: Kluwer Academic Publishers.
- Osburn, C. L., N. J. Anderson, M. J. Leng, C. D. Barry, and E. J. Whiteford. 2019. Stable isotopes reveal independent carbon pools across an Arctic hydro-climatic gradient: Implications for the fate of carbon in warmer and drier conditions. *Limnol. Oceanogr.: Lett.* **4**: 205–213. doi:10.1002/lo2.10119
- Osterholz, H., J. Niggemann, H. A. Giebel, M. Simon, and T. Dittmar. 2015. Inefficient microbial production of refractory dissolved organic matter in the ocean. *Nat. Commun.* **6**: 1–8. doi:10.1038/ncomms8422
- Pacheco, F. S., F. Roland, and J. A. Downing. 2014. Eutrophication reverses whole-lake carbon budgets. *Inland Waters* **4**: 41–48. doi:10.5268/IW-4.1.614
- Paerl, H. W., and T. G. Otten. 2013. Blooms bite the hand that feeds them. *Science* **342**: 433–434. doi:10.1126/science.1245276
- Patriarca, C., J. Bergquist, P. J. R. Sjöberg, L. Tranvik, and J. A. Hawkes. 2018. Online HPLC-ESI-HRMS method for the analysis and comparison of different dissolved organic matter samples. *Environ. Sci. Technol.* **52**: 2091–2099. doi:10.1021/acs.est.7b04508
- Pérez, M. T., and R. Sommaruga. 2006. Differential effect of algal- and soil-derived dissolved organic matter on alpine lake bacterial community composition and activity. *Limnol. Oceanogr.* **51**: 2527–2537. doi:10.4319/lo.2006.51.6.2527
- Perminova, I. V., and others. 2014. Molecular mapping of sorbent selectivities with respect to isolation of arctic dissolved organic matter as measured by Fourier transform mass spectrometry. *Environ. Sci. Technol.* **48**: 7461–7468. doi:10.1021/es5015423
- Petras, D., and others. 2017. High-resolution liquid chromatography tandem mass spectrometry enables large scale molecular characterization of dissolved organic matter. *Front. Mar. Sci.* **4**. doi:10.3389/fmars.2017.00405
- Pivokonsky, M., J. Safarikova, M. Baresova, L. Pivokonska, and I. Kopecka. 2014. A comparison of the character of algal extracellular versus cellular organic matter produced by cyanobacterium, diatom and green alga. *Water Res.* **51**: 37–46. doi:10.1016/j.watres.2013.12.022
- Powers, L. C., N. Hertkorn, N. McDonald, P. Schmitt, R. Del Vecchio, N. V. Blough, and M. Gonsior. 2019. *Sargassum* sp. act as a large regional source of marine dissolved organic carbon and polyphenols. *Global Biogeochem. Cycles* **33**: 1423–1439. doi:10.1029/2019GB006225
- Raeke, J., O. J. Lechtenfeld, M. Wagner, P. Herzsprung, and T. Reemtsma. 2016. Selectivity of solid phase extraction of freshwater dissolved organic matter and its effect on ultra-high resolution mass spectra. *Environ. Sci. Process. Impacts* **18**: 918–927. doi:10.1039/c6em00200e
- Riedel, T., and T. Dittmar. 2014. A method detection limit for the analysis of natural organic matter via Fourier transform ion cyclotron resonance mass spectrometry. *Anal. Chem.* **86**: 8376–8382. doi:10.1021/ac501946m
- Rippka, R., J. Deruelles, and J. B. Waterbury. 1979. Generic assignments, strain histories and properties of pure cultures of cyanobacteria. *J. Gen. Microbiol.* **111**: 1–61. doi:10.1099/00221287-111-1-1
- Ritson, J. P., N. J. D. Graham, M. R. Templeton, J. M. Clark, R. Gough, and C. Freeman. 2014. The impact of climate change on the treatability of dissolved organic matter (DOM) in upland water supplies: A UK perspective. *Sci. Total Environ.* **473–474**: 714–730. doi:10.1016/j.scitotenv.2013.12.095
- Sarmiento, H., and J. M. Gasol. 2012. Use of phytoplankton-derived dissolved organic carbon by different types of bacterioplankton. *Environ. Microbiol.* **14**: 2348–2360. doi:10.1111/j.1462-2920.2012.02787.x
- Stanier, R. Y., R. Kunisawa, M. Mandel, and G. Cohen-Bazire. 1971. Purification and properties of unicellular blue-green algae (order Chroococcales). *Bacteriol. Rev.* **35**: 171–205. doi:10.1128/mbr.35.2.171-205.1971
- Stoll, N., E. Schmidt, and K. Thurow. 2006. Isotope pattern evaluation for the reduction of elemental compositions assigned to high-resolution mass spectral data from electrospray ionization Fourier transform ion cyclotron resonance mass spectrometry. *J. Am. Soc. Mass Spectrom.* **17**: 1692–1699. doi:10.1016/j.jasms.2006.07.022

- Teeling, H., and others. 2012. Substrate-controlled succession of marine bacterioplankton populations induced by a phytoplankton bloom. *Science* **336**: 608–611. doi:[10.1126/science.1218344](https://doi.org/10.1126/science.1218344)
- Toming, K., and others. 2013. Contributions of autochthonous and allochthonous sources to dissolved organic matter in a large, shallow, eutrophic lake with a highly calcareous catchment. *Limnol. Oceanogr.* **58**: 1259–1270. doi:[10.4319/lo.2013.58.4.1259](https://doi.org/10.4319/lo.2013.58.4.1259)
- Wells, M. L., and others. 2015. Harmful algal blooms and climate change: Learning from the past and present to forecast the future. *Harmful Algae* **49**: 68–93. doi:[10.1016/j.hal.2015.07.009](https://doi.org/10.1016/j.hal.2015.07.009)
- Witt, M., J. Fuchser, and B. P. Koch. 2009. Fragmentation studies of fulvic acids using collision induced dissociation fourier transform ion cyclotron resonance mass spectrometry. *Anal. Chem.* **81**: 2688–2694. doi:[10.1021/ac802624s](https://doi.org/10.1021/ac802624s)
- Woods, G. C., M. J. Simpson, P. J. Koerner, A. Napoli, and A. J. Simpson. 2011. HILIC-NMR: Toward the identification of individual molecular components in dissolved organic matter. *Environ. Sci. Technol.* **45**: 3880–3886. doi:[10.1021/es103425s](https://doi.org/10.1021/es103425s)
- Zark, M., J. Christoffers, and T. Dittmar. 2017. Molecular properties of deep-sea dissolved organic matter are predictable by the central limit theorem: Evidence from tandem FT-ICR-MS. *Mar. Chem.* **191**: 9–15. doi:[10.1016/j.marchem.2017.02.005](https://doi.org/10.1016/j.marchem.2017.02.005)
- Zhao, M., D. Qu, W. Shen, and M. Li. 2019. Effects of dissolved organic matter from different sources on *Microcystis aeruginosa* growth and physiological characteristics. *Ecotoxicol. Environ. Saf.* **176**: 125–131. doi:[10.1016/j.ecoenv.2019.03.085](https://doi.org/10.1016/j.ecoenv.2019.03.085)
- Zheng, X., and others. 2017. Chemical Science database for over 500 metabolites and xenobiotics. *Chem. Sci.* **8**: 7724–7736. doi:[10.1039/c7sc03464d](https://doi.org/10.1039/c7sc03464d)
- Zhou, Y., L. Zhou, Y. Zhang, J. Garcia de Souza, D. C. Podgorski, R. G. M. Spencer, E. Jeppesen, and T. A. Davidson. 2019. Autochthonous dissolved organic matter potentially fuels methane ebullition from experimental lakes. *Water Res.* **166**: 115048. doi:[10.1016/j.watres.2019.115048](https://doi.org/10.1016/j.watres.2019.115048)

Acknowledgments

The authors thank Andrea Balderrama and Temitope Odunayo Nwachukwu for assistance in the laboratory. Funding was provided by the Knut and Alice Wallenberg Foundation via a larger collaborative grant to L.J.T. (KAW 2013.0091), Kungl. Vetenskapsakademiens Stiftelser (CR2019-0060 to S.L.G.), and the Swedish Research Council (grants 2018-04618 to J.A.H.; 2017-04422 to S.B.; 2015-4870 to J.B.).

Conflict of Interest

None declared.

Submitted 30 March 2020

Revised 28 July 2020

Accepted 17 September 2020

Associate editor: Hans-Peter Grossart